PAPER

Check for updates

Sustainable carbonaceous nanomaterial supported palladium as an efficient ligand-free heterogeneouscatalyst for Suzuki–Miyaura coupling†

Apoorva Shetty,[ab] Dhanya Sunil, [c] Thitima Rujiralai, [d] Sanjeev P. Maradur, [e] Abdullah N. Alodhayb [f] and Gurumurthy Hegde [*abe]

A novel ligand-free heterogeneous catalyst was synthesized *via* pyrolysis of *Samanea saman* pods to produce carbon nanospheres (SS-CNSs), which served as a carbon support for immobilizing palladium nanoparticles through an *in situ* reduction technique (Pd/SS-CNS). The SS-CNSs effectively integrated 3% of Pd on their surfaces with no additional activation procedures needed. The nanomaterials obtained underwent thorough characterization employing various techniques such as FT-IR, XRD, FE-SEM, TEM, EDS, ICP-AES, and BET. Subsequently, the efficiency of this Pd/SS-CNS catalyst was assessed for the synthesis of biaryl derivatives *via* Suzuki coupling, wherein different boronic acids were coupled with various aryl halides using an environmentally benign solvent mixture of EtOH/H_2O and employing only 0.1 mol% of Pd/SS-CNS. The catalytic system was conveniently recovered through centrifugation and demonstrated reusability without any noticeable decline in catalytic activity. This approach offers economic viability, ecological compatibility, scalability, and has the potential to serve as an alternative to homogeneous catalysis.

Introduction

Amidst the array of metal catalysts, palladium-based homogeneous complexes stand out for their exceptional performance in Suzuki coupling reactions.[1,2] While these catalysts demonstrate remarkable efficacy, challenges in separating the catalyst from the reaction environment and reusing it hinder their large-scale industrial applications. To address these issues, researchers have devised novel heterogeneous catalytic systems.[3–5] However, most of the proposed heterogeneous palladium-catalyst systems for Suzuki coupling reactions involve intricate and time-consuming work-up procedures, incurring high costs and complex synthesis processes. Consequently, there is an urgent

need for further research aimed at designing heterogeneous Pd nanocatalysts that combine favorable activity, stability, and reusability. The advancement of such catalysts holds immense potential for driving progress in the chemical and pharmaceutical industries. A broad spectrum of support materials, spanning both inorganic and organic varieties such as mesoporous silica, alumina, zeolites, metal–organic frameworks (MOFs), supramolecular polymers, alongside various carbon-based materials like graphite, carbon black, and activated carbon, find utility in dispersing active components across numerous catalytic processes.[6–12] However carbon, distinguished for its substantial specific surface area, notable porosity, excellent electron conductivity, and relative chemical inertness, has emerged as a prominent support material for chemical transformation reactions. An additional advantage lies in its capacity to be sourced from residual biomass, thus contributing to the overall reduction of the carbon footprint in biomass transformation processes. Furthermore, carbon materials can undergo chemical functionalization and/or be adorned with metallic nanoparticles (NPs) and enzymes to confer or enhance novel catalytic activities. Leveraging these attributes, porous carbon materials demonstrate promise as supports for heterogeneous catalysis when compared with alternative supports.[13]

The emergence of carbon nanostructures, notably carbon nanotubes (CNTs) and carbon nanofibers (CNFs), has sparked substantial efforts in their synthesis, characterization,

[a]Department of Chemistry, CHRIST (Deemed to Be University), Hosur Road, Bangalore 560029, India

[b]Centre for Advanced Research and Development (CARD), CHRIST (Deemed to Be University), Hosur Road, Bangalore 560029, India. E-mail: murthyhegde@gmail.com

[c]Department of Chemistry, Manipal Institute of Technology, Manipal Academy of Higher Education, Manipal, Karnataka 576104, India

[d]Center of Excellence for Innovation in Chemistry, Division of Physical Science, Faculty of Science, Prince of Songkla University, Hat Yai, Songkhla, 90112, Thailand

[e]Materials Science & Catalysis Division, Poornaprajna Institute of Scientific Research (PPISR), Bidalur Post, Devanahalli, Bengaluru 562164, Karnataka, India

[f]Department of Physics and Astronomy, College of Science, King Saud University, Riyadh 11451, Saudi Arabia

† Electronic supplementary information (ESI) available: ^{1}H NMR, ^{13}C NMR and, GC-MS data of compounds (S1–S29). See DOI: https://doi.org/10.1039/d4na00116h

modification in the surface properties, and practical applications. These structures have found utility across diverse technological domains, including catalysis, adsorption,[14–16] hydrogen storage,[17] and electronics.[18] Beyond the filamentous arrangement giving rise to CNTs and CNFs, carbon can adopt alternative bonding configurations, yielding structures with distinct properties. For instance, the combination of pentagonal and heptagonal carbon rings leads to the formation of carbon nanospheres (CNSs). This innovative nanostructure has recently attracted significant research interest.[19] In its spherical configuration, the graphite sheets do not form closed shells; instead, they manifest as waving flakes that conform to the sphere's curvature, leading to numerous exposed edges at the surface. Unlike in C60, which is chemically inert, these unsealed graphitic flakes exhibit dangling bonds[20] that are highly reactive, which are believed to amplify the surface reactions. Consequently, CNSs emerges as a promising candidate for catalytic and adsorption applications.[21] CNSs can be employed as a catalyst support, offering several advantages over activated carbons and CNTs such as facile synthesis devoid of catalysts, tunable physical properties (in terms of size, purity, porosity), and attaining high yields of pure materials.

Although the utilization of CNSs as a catalyst supports various advantages, only limited reports exist in this domain. Generally, carbon nanospheres are produced through catalytic[22] or thermal decomposition[23] of hydrocarbon feedstocks, as well as hydrothermal,[24] template,[25] coating,[26] or metathesis routes.[27] However, the utilization of biomaterials in carbon nanosphere synthesis remains largely unexplored.[28,29] Hence, extensive research is underway to focus on crafting this novel carbon structure from the biowaste that meets diverse requirements, encompassing ease of availability, cost-effectiveness, sustainability, and inert characteristics. Furthermore, it is crucial for the carbon material to effectively immobilize metal nanoparticles, such as palladium, while preventing their leaching into the solution. Additionally, the carbon support should establish a robust heterogeneous catalytic system with the metal, enabling easy recyclability and reusability.

In this study, a novel and renewable ligand-free heterogeneous catalyst Pd/SS-CNSs derived from *Samanea saman* pods was developed. The *Samanea saman* pods contains lignocellulosic content of about ~45% (cellulose ~ 14%, hemicellulose ~ 13%, lignin ~ 18%)[30–32] based on % DM basis which serves as the source of carbon in the process of synthesizing the carbon nanospheres. The synthesis involved the pyrolysis technique to create SS-CNSs, followed by the immobilization of palladium nanoparticles using an *in situ* reduction of Pd(ɪɪ) precursor.

The Pd/SS-CNSs catalyst was then applied to test its catalytic activity for the well-known Suzuki–Miyaura coupling reaction, specifically focusing on the reaction conditions involving 4-bromophenol and phenylboronic acid. The optimization of the solvent, base, and catalyst loading was done to enhance the efficiency of the reaction. Furthermore, the study proposed a catalytic mechanism for the Suzuki coupling reaction over the synthesized Pd/SS-CNSs catalyst based on various characterizations of the catalyst and experimental results. This research

opens up new possibilities for more efficient and cost-effective catalytic systems in Suzuki coupling reaction.

Experimental

Materials and methods

The aryl halides and boronic acids required for the synthesis of the C–C coupled compounds were procured from Avra Synthesis Pvt Ltd and were used as received without any further purification. Ethanol was obtained from Finar Chemicals. All others chemicals, such as $PdCl_2$, potassium carbonate, sodium carbonate were procured from Chempure.

Preparation of materials

Synthesis of the carbon nanospheres (SS-CNSs). The carbon nanospheres were prepared using a one-step pyrolysis technique (Fig. 1a). The biowaste precursor *Samanea saman* pods was washed thoroughly with water, sun-dried, powdered, and sieved using a sieve to 150 μm. The ground precursor was taken in a silica crucible and subjected to pyrolysis in a N_2 atmosphere at 800 °C in a quartz tube furnace. The nitrogen flow was kept constant throughout the synthesis. The pyrolysed carbon was then rinsed with 0.1 N HCl, followed by thorough washing with water, and subsequently dried before being utilized for further studies. More details about the synthetic procedure can be found in our earlier articles.[29] Although we synthesized CNSs at various temperatures (for examples 400, 600, 800 and 1000 °C) but 800 °C attained excellent performance interms of size, shape, surface area and carbon content. Due to this reason CNSs synthesized at 800 °C has been chosen for further work.

Preparation of Pd-supported CNSs (Pd/SS-CNSs). The synthesized SS-CNSs (500 mg) was taken in a 100 mL beaker containing 10 mL of distilled water. The mixture was heated to 80 °C for 30 min. To this a suspension of $PdCl_2$ in HCl was added. After stirring the mixture for 20 min, 0.2 mL portion of formaldehyde (40% solution in water) was slowly introduced into the reaction mixture to facilitate the reduction of Pd(ɪɪ) to Pd(0). Following an additional 10 min of continuous stirring, the resulting mixture was then neutralized using a 30% NaOH solution. The suspension was left to settle, then filtered, meticulously rinsed with distilled water and subsequently dried to obtain Pd-supported CNSs(Pd/SS-CNSs) (Fig. 1b).

Material characterization

To examine the microstructure of SS-CNSs and Pd/SS-CNSs, images taken using a transmission electron microscope (TEM) (JEOL JEM-2010, Japan) were acquired. To determine the morphology of the samples and confirm the presence and relative abundance of elements, field emission scanning electron microscopy (FESEM) and EDS analysis was performed with (Apero Thermo Fisher Scientific, USA) operated at an accelerating voltage of 20.0 kV. X-ray diffraction (XRD) patterns were obtained from Rigaku Miniflex 600 (Rigaku, Japan) employing Cu-Kα radiation. Inductively coupled plasma analysis (ICPAES), ARCOS (SPECTRO Analytical Instruments GmbH, Germany) was used to quantify the elemental concentration of Pd in Pd/SS-CNSs. For the chemical
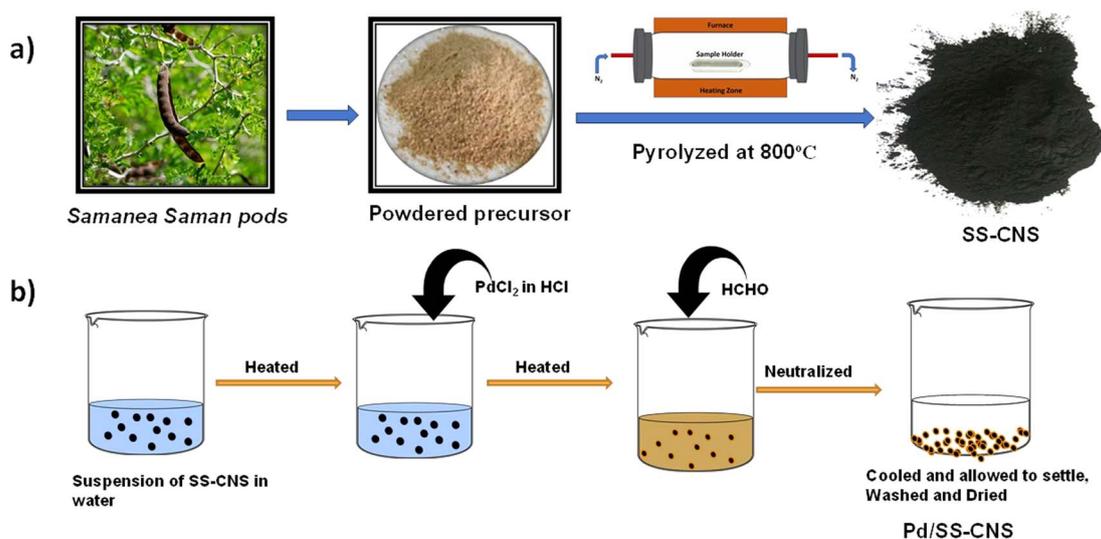
Fig. 1 Synthesis of SS-CNSs (a), synthesis of Pd/SS-CNSs(b).

structure and composition analysis of the synthesized Pd/SS-CNSs nanomaterial, Fourier-transformed infrared (FT-IR) spectra were recorded with IRSpirit-L (SHIMADZU, Japan). During the catalytic study of Pd/SS-CNSs, the samples of coupled products were analyzed by gas chromatography (GCMS-QP2010 SE, SHIMADZU, Japan). The isolated compounds were characterized by ^{1}H and ^{13}C NMR spectroscopy (Bruker Ascend 400 MHz) using dimethyl sulfoxide-d$_6$ (DMSO-D$_6$) as solvent.

General procedure for the Suzuki–Miyaura coupling reaction using Pd/SS-CNSs catalyst

A solution containing aryl halide (1.0 mmol), aryl boronic acid (1.2 mmol), K$_2$CO$_3$ (2.0 mmol), Pd/SS-CNSs (0.1 mol%), and EtOH/H$_2$0 (2 : 1) was stirred at 70 °C. The progress of the reaction was timely monitored with TLC. At the completion of the reaction, the reaction mixture was allowed to cool to room temperature. Into the reaction mixture 10 mL of H$_2$O and 10 mL of EtOAc were added. The catalyst was separated using centrifugation, and the organic layer was extracted with EtOAc (3 × 10 mL) using a separating funnel and dried over anhydrous Na$_2$SO$_4$. The organic solvent was

evaporated under reduced pressure to obtain the crude. The products were isolated using the column chromatography method on silica gel (60–120 mesh) using EtOAc : hexane as mobile phase. The ^{1}H NMR spectra and GCMS was recorded to confirm the formation of product.

Procedure for the reuse of the catalyst

Following the completion of the reaction, 5 mL of EtOAc was added to the reaction mixture and stirred for 5 minutes. The catalyst was then isolated from the mixture through centrifugation. Next, the isolated Pd/SS-CNSs catalyst was washed with ethanol and dried under vacuum. This recovered catalyst was subsequently employed for another reaction run, showcasing its reusability and suitability for multiple cycles of the reaction.

Results and discussion

Characterization of the Pd/SS-CNSs catalyst

Fig. 1 outlines the systematic procedure for synthesizing the Pd/SS-CNSs catalyst. The biowaste *Samanea saman* pods,
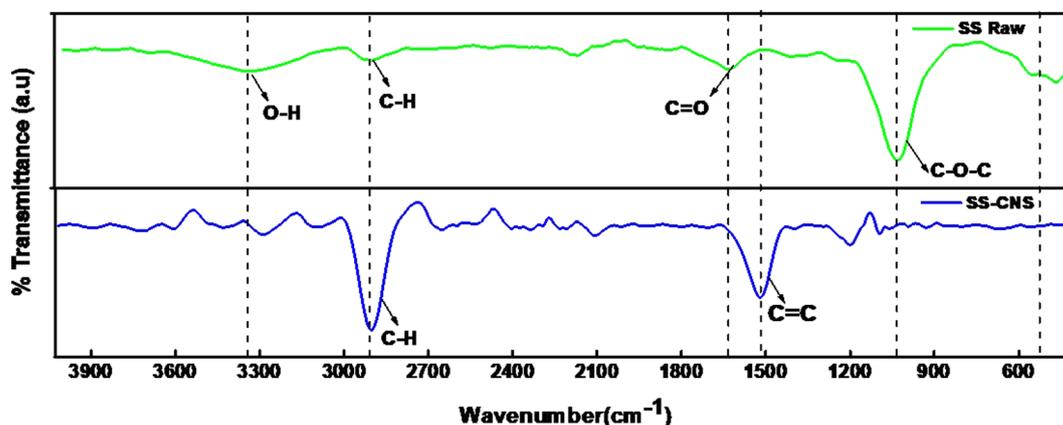

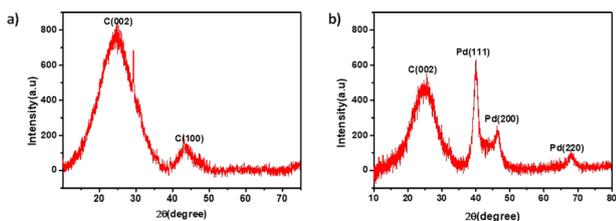Fig. 2 FTIR spectra of SS raw and SS-CNSs.

Fig. 3 X-ray diffraction pattern of SS-CNS (a), Pd/SS-CNS (b).

containing 45% lignocellulosic content, was utilized as the natural carbon source for generating carbon nanospheres (CNSs) which were produced through a one-step pyrolysis technique under nitrogen atmosphere. Subsequently, the heterogeneous catalytic system based on palladium (Pd) was fabricated. This involved the reduction of $PdCl_2$ using formaldehyde as a reducing agent, resulting in the transformation of Pd(II) to Pd(0). This method ensures that catalysts reduced with formaldehyde do not carry adsorbed hydrogen and exhibit reduced pyrophoric properties.[33]

In the analysis of the FTIR spectra of SS-raw and SS-CNSs (Fig. 2) distinct peaks were identified. In the precursor (SS-raw), a broad peak was identified at 3415 cm^{-1}, indicating the presence of OH stretching vibration.[34] Additionally, a peak at 2889 cm^{-1} was attributed to C–H stretching vibration,[35] while the band around 1633 cm^{-1} signified the carboxyl group (C=O), indicating a significant oxygen content in the samples.[36] The intense band at 1033 cm^{-1} may arise from the C–O–C glycosidic linkage of hemicellulose and cellulose moieties, or it can be also due to the C–O stretching vibration in ether, ester, and phenolic groups.[34,37] In contrast, for SS-CNSs, the elevated synthesis temperature of 800 °C resulted in a notable reduction in oxygen content. This was reflected in the spectrum by the emergence of two prominent peaks at 2889 cm^{-1} and 1507 cm^{-1}, indicative of C–H stretching vibration and C=C stretching vibration, respectively.[36]

The Fig. 3 displays the X-ray diffraction (XRD) patterns for both the synthesized SS-CNSs and Pd/SS-CNSs. In the XRD profile of SS-CNSs, noticeable broad peaks were observed at approximately 24° and 44°, corresponding to the (002) and (100) lattice planes of carbon, respectively.[38] The broad nature of these peaks suggested the amorphous nature of the carbon material. Furthermore, the XRD pattern of Pd/SS-CNSs substantiated the presence of Pd particles on the carbon
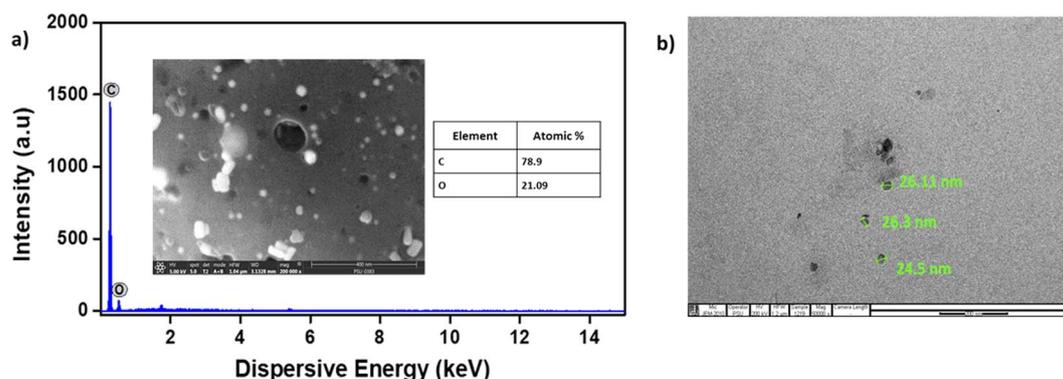

Fig. 4 SEM images of SS-CNS along with EDS mapping of composition elements (a), TEM image of SS-CNS (b).
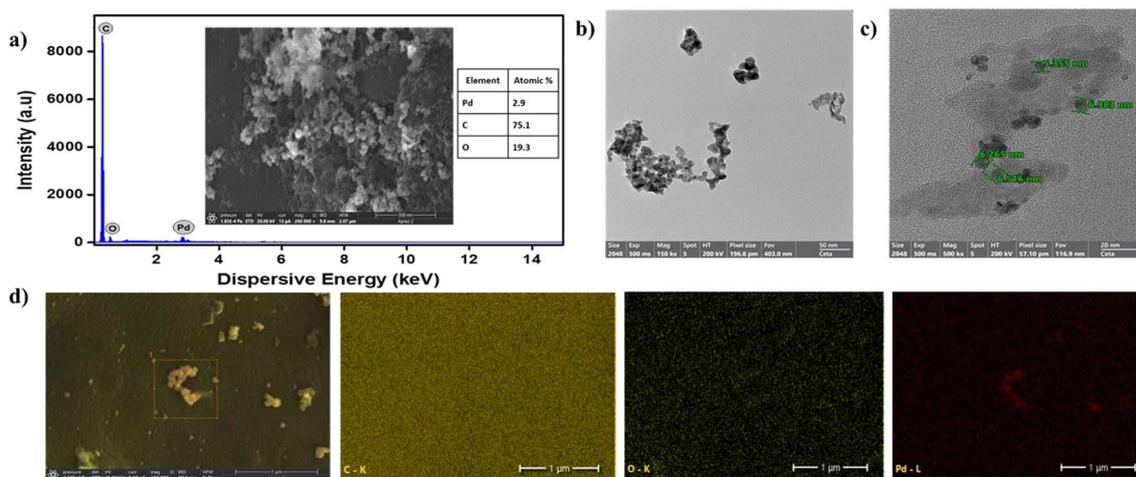

Fig. 5 FESEM image along with EDS plot of Pd/SS-CNSs (a), TEM images of Pd/SS-CNSs (b and c), Pd/SS-CNSs; elemental mapping of composition elements C, O and Pd (d).
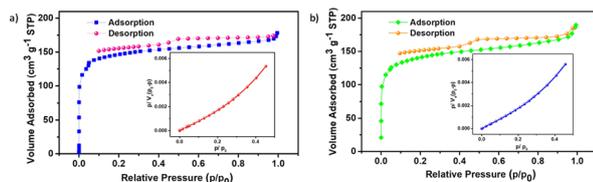
Fig. 6   BET adsorption–desorption isotherm graph of SS-CNSs; BET plot of the nitrogen adsorption shown in the inset (a), Pd/SS-CNSs; BET plot of the nitrogen adsorption shown in the inset (b).

substrate. In addition to the broad peak at approximately 24°, indicative of the (002) facet of amorphous carbon, three distinct and prominent peaks were identified at $2\theta = 39.7°$, 45.6°, and 67.5°, attributing to the (111), (200), and (220) facets of the Pd particles.[39]

The structural characteristics of SS-CNSs and Pd/SS-CNSs were initially assessed through FESEM. In Fig. 4a, CNSs displayed a spherical morphology and the EDS analysis of SS-CNSs indicated that carbon constituted approximately 79% of the composition. The FESEM-EDS image (Fig. 5a) of Pd/SS-CNSs further affirmed the retention of the spherical morphology of the CNSs in addition to the presence of Pd (2.9%) in the catalyst along with a 75% carbon content. Elemental mapping demonstrated a homogeneous distribution of palladium on the carbon surface (Fig. 5d). The spherical morphology of both SS-CNSs and Pd/SS-CNSs was further examined using TEM (Fig. 4b and 5b, c). Fig. 4b illustrates the spherical shape of CNSs with an average diameter of 24–26 nm. Upon closer inspection in magnified TEM images (Fig. 5b and c), the presence of Pd particles on the CNSs surface was evident. These images also revealed Pd particles of approximately 5–7 nm in size (Fig. 5c) situated on the carbon spheres, which were arranged randomly along the edges and displayed wave-flake like features.

The Brunauer–Emmett–Teller (BET) method was used to assess the surface area of the synthesized catalyst. N_2 adsorption–desorption isotherm of SS-CNSs (Fig. 6a) and Pd/SS-CNSs (Fig. 6b) reveals type IV hysteresis with a BET surface area of 495 m^2 g^{-1} with a pore volume of 0.2685 cm^3 g^{-1} for SS-CNSs and BET surface area of 523 m^2 g^{-1} with a pore volume of 0.289 cm^3 g^{-1} for Pd/SS-CNSs. The mean pore diameters are 2.16 nm and 2.2 nm respectively. These results indicate that there is not much change in the surface area and pore diameter of the catalyst after incorporation of Pd. The catalyst has hence demonstrated mesoporous nature with relatively good surface area.

Catalytic activity of Pd/SS-CNSs in Suzuki–Miyaura coupling

Optimization studies. In continuation of the efforts to test the applicability of the synthesized Pd/SS-CNSs as a heterogeneous catalyst in the Suzuki coupling reaction, after thorough characterization of the catalyst, optimization studies were carried out considering the coupling of 4-bromophenol with phenylboronic acid as a model reaction system. To provide more sustainable reaction conditions, a series of reactions were carried out with various solvents, bases, and catalyst loadings.

All the results obtained during the process are listed in the Table 1. The selection of solvents will greatly influence the result of the Suzuki coupling reaction. Hence, the choice of solvent emerged as one of the significant factors in the study. For this investigation, two alcoholic solvents: MeOH and EtOH/H_2O (2 : 1), as well as two aprotic polar solvents commonly employed in Pd-catalyzed coupling reactions N,N-dimethylformamide (DMF) and tetrahydrofuran (THF) were evaluated. Throughout these experiments, both the base (Na_2CO_3) and the temperature (70 °C) were held constant. The experimental results, as detailed in the Table 1 (entries 1–5), demonstrated promising conversion rates (89%) for the EtOH/H_2O system, whereas the DMF system exhibited inadequate conversion. On the other hand, the MeOH and THF solvent systems did not yield favorable outcomes in promoting the desired coupling reaction. The reaction, when performed solely in EtOH, no significant product conversion was observed, with the base (Na_2CO_3) remaining insoluble in the reaction mixture. Hence, the addition of water to the system was crucial to promote the solubility of the base and also for the better dispersion of the catalyst, facilitating the formation of the desired product. Owing to the higher conversion rate achieved with the EtOH/H_2O (ethanol/water) solvent system, which also aligns with environmentally friendly solvent choices, this solvent system was selected as the optimal choice for subsequent investigations.

In the next stage, the examination of bases, which plays a critical role in the transmetallation step and which is responsible for interacting with phenylboronic acid to generate phenyl borate ($Ar_2B(OH)_2X$) thereby activating the boronic acid for Suzuki coupling was carried out. Consequently, the impact of various bases, including Na_2CO_3, K_2CO_3, Cs_2CO_3, and K_3PO_4, (refer to Table 1, entries 5–8) was explored within the chosen solvent system. Among these bases, K_2CO_3 exhibited the highest efficacy, achieving a remarkable 95% conversion within the EtOH/H_2O system.

Table 1   Optimization of the reaction conditions for the Suzuki coupling of 4-bromophenol with phenylboronic acid catalyzed by Pd/SS-CNSs[a]

Sl. no.	Solvent	Base	Catalyst loading (Pd mol%)	Product conversion[b]
1	MeOH	Na_2CO_3	0.5	No reaction
2	THF	Na_2CO_3	0.5	No reaction
3	DMF	Na_2CO_3	0.5	3.6%
4	EtOH	Na_2CO_3	0.5	No reaction
5	EtOH/H_2O	Na_2CO_3	0.5	89.16%
6	EtOH/H_2O	K_2CO_3	0.5	95.35%
7	EtOH/H_2O	Cs_2CO_3	0.5	40.5%
8	EtOH/H_2O	K_3PO_4	0.5	No reaction
9	EtOH/H_2O	K_2CO_3	0.3	88.38%
10	EtOH/H_2O	K_2CO_3	0.2	91.3%
11	**EtOH/H_2O**	**K_2CO_3**	**0.1**	**91.6%**

[a] Reaction conditions: 4-bromophenol (1.0 mmol), phenyl boronic acid (1.0 mmol), temperature 70 °C, time 1 h. [b] Product conversion based on GCMS analysis.

Table 2 Suzuki–Miyaura reactions between phenylboronic acids and aryl halides catalyzed by Pd/SS-CNS
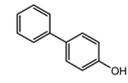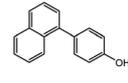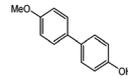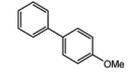
Conditions: Pd/SS-CNS (0.1mol%), K_2CO_3(2.0 eq), 70°C, EtOH/H_2O (2:1), Time
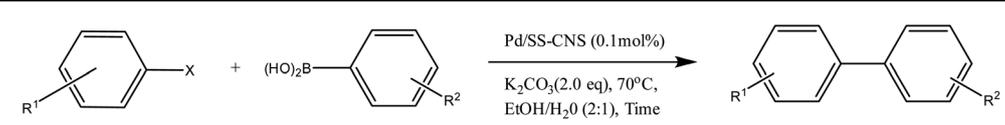
Entry	R^1	X	Boronic acid	Product		Time (min)	Isolated yield (%)
1	4-OH	Br	Phenyl boronic acid		**1f**	60	96
2	4-OH	Br	Naphthalen-1-yl boronic acid		**2f**	90	82
3	4-OH	Br	(4-Methoxyphenyl)boronic acid		**3f**	90	91
4	4-OMe	Br	Phenylboronic acid		**4f**	240	85
5	4-OMe	Br	Naphthalen-1-ylboronic acid		**5f**	240	62
6	4-OMe	Br	(4-Methoxyphenyl)boronic acid		**6f**	240	73
7	H	Br	Phenylboronic acid		**7f**	60	93
8	H	Br	Naphthalen-1-ylboronic acid		**8f**	60	78
9	H	Br	(4-Methoxyphenyl)boronic acid		**9f**	60	79
10	4-NO_2	Br	Phenylboronic acid		**10f**	120	85
11	4-NO_2	Br	Naphthalen-1-ylboronic acid		**11f**	180	78
12	4-NO_2	Br	(4-Methoxyphenyl)boronic acid		**12f**	100	93
13	4-CN	Br	Phenylboronic acid		**13f**	60	93
14	4-CN	Br	Naphthalen-1-ylboronic acid		**14f**	60	87
15	4-CN	Br	(4-Methoxyphenyl)boronic acid		**15f**	60	95
16	4-Me	Br	Phenylboronic acid		**16f**	60	85
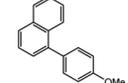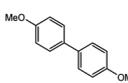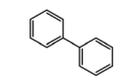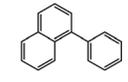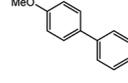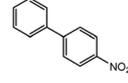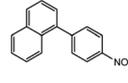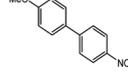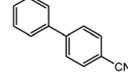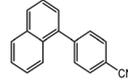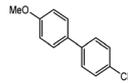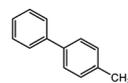
Table 2 (*Contd.*)

Entry	R^1	X	Boronic acid	Product		Time (min)	Isolated yield (%)
17	4-Me	Br	Naphthalen-1-ylboronic acid		**17f**	60	86
18	4-Me	Br	(4-Methoxyphenyl)boronic acid		**18f**	60	97
19	4-CHO	Br	Phenylboronic acid		**19f**	60	89
20	4-CHO	Br	Naphthalen-1-ylboronic acid		**20f**	70	92
21	4-CHO	Br	(4-Methoxyphenyl)boronic acid		**21f**	50	98
22	H	I	Phenylboronic acid		**22f**	20	88
23	H	I	Naphthalen-1-ylboronic acid		**23f**	20	87
24	H	I	(4-Methoxyphenyl)boronic acid		**24f**	20	90
25	4-OMe	I	Phenylboronic acid		**25f**	20	82
26	4-OMe	I	Naphthalen-1-ylboronic acid		**26f**	20	81
27	4-OMe	I	(4-Methoxyphenyl)boronic acid		**27f**	20	94
28	H	Cl	Phenylboronic acid		**28f**	270	62

Further experiments were performed to optimize the catalyst loading. For this study, Pd loadings of 0.5 mol%, 0.3 mol%, 0.2 mol% and 0.1 mol% were considered (refer to Table 1, entries 6 and 9–11). After examining the reactions at different catalyst loadings, a Pd loading of 0.1 mol% was identified as the most effective catalyst amount for further studies as it delivered promising product conversion while utilizing the least loading of palladium among the considered dosages. Besides that, increasing the mol% of the catalyst did not exert a substantial impact on the catalytic performance in the current study. This observation can be ascribed to the well-dispersed nature of Pd nanoparticles across the surface of carbon nanospheres, facilitating efficient catalytic activity.

Reactions. To assess the versatility of the Pd/SS-CNSs catalyst, an investigation was conducted on the Suzuki coupling reaction involving a diverse array of substrates under optimized conditions. The outcomes of these experiments are detailed in Table 2. The results highlight that a wide range of aryl bromides successfully underwent reactions with phenylboronic acid, naphthalen-1-ylboronic acid, and (4-methoxyphenyl)boronic acid, yielding the desired products with high efficiency. Among the various aryl bromides examined, those incorporating

electron-withdrawing substituents like –NO_2, –CHO, and –CN (as indicated in Table 2 entries 10–15 and 19–21) exhibited particularly good yields often accompanied by shorter reaction times. In contrast, aryl bromides containing electron-releasing substituent such as –OCH_3, –OH, and –CH_3 in the *para* position necessitated extended reaction durations to achieve satisfactory yields (as seen in Table 2 entries 1–6 and 16–18). Furthermore, a noteworthy observation was made, pairings of aryl bromides possessing electron-withdrawing groups with boronic acids featuring electron-donating functionalities demonstrated both shorter reaction times and improved yields compared to their counterparts (notably shown in Table 2 entries 12, 15, and 21).

The successful application of the Pd/SS-CNSs catalytic system extended to reactions involving aryl iodides and aryl boronic acids, as demonstrated in Table 2 entries 22–27. In these cases, favorable yields of the desired products were achieved, often in a shorter time frame compared to the coupling of aryl bromides. This increased reactivity of aryl iodides in Suzuki coupling can be attributed to their lower electronegativity (iodo group: 2.66) and a relatively lower bond dissociation energy for the C–I bond (64 kcal mol^{-1}) compared to the C–Br bond (79 kcal mol^{-1}). To broaden the study's scope, the reaction between chlorobenzene and phenylboronic acid was investigated. However, in contrast to reactions involving aryl bromides and aryl iodides, the reactions with the chloro derivative exhibited prolonged reaction times and yielded fewer products (Table 2 entry 28). This diminished yield could be ascribed to the robust strength of the C–Cl bond, characterized by a high bond dissociation energy of 96 kcal mol^{-1}. The coupled products were characterized using GCMS, ^1H NMR and ^{13}C NMR and the details are given in ESI (S1–S28).†

Recyclability, stability and heterogeneity test of Pd/SS-CNSs. The recyclability of the Pd/SS-CNSs catalyst was evaluated in the context of the Suzuki coupling reaction between 4-bromophenol and phenylboronic acid in the optimized reaction conditions. After the first cycle, yielded 92% of the desired product, the catalyst was then retrieved by centrifugation, washed with H_2O and EtOH, and dried. The recovered Pd/SS-CNSs catalyst was then employed in subsequent reaction runs under identical conditions. The results as illustrated in Fig. 7a, showed that in

the fifth run, Pd/SS-CNS achieved a product yield of 75%. This significant yield after multiple reaction cycles demonstrates the recyclability of Pd/SS-CNSs, making it a promising and efficient catalyst for the Suzuki reaction.

The heterogeneity of Pd/SS-CNSs was a crucial parameter under investigation, particularly in terms of leaching behavior. Through ICP-AES analysis of the recycled catalyst, it was observed that the palladium content in the used catalyst remained at 2.4%, while the unused catalyst showed a palladium content of 3% in ICP-AES analysis. This finding indicates that there was no significant leaching of palladium during the reaction, affirming the stability of Pd/SS-CNSs under the reaction conditions. The XRD analysis (Fig. 7b) also indicated the characteristic peaks for palladium and carbon. The FTIR spectra (Fig. 7d) recorded for the Pd/SS-CNS and Pd/SS-CNS-R also show no significant change in the spectra, two peaks at 2889 cm^{-1} and 1507 cm^{-1}, indicative of C–H stretching vibration and C=C stretching vibration were present in both the samples. Furthermore, examination of the morphology of the catalyst using FESEM (Fig. 7c) after recycling revealed no substantial changes. These results strongly suggests that Pd/SS-CNSs is both recyclable and stable during the reaction.

To further confirm the heterogeneous nature of Pd/SS-CNSs, a hot filtration test was carried out on the reaction mixture of 4-bromophenol with phenylboronic acid, following the optimized conditions. The test showed partial conversion into product after 30 minutes of reaction time. When the catalyst was separated, and the reaction was continued for an additional 120 minutes without the catalyst, the GC-MS analysis confirmed that there was no significant increase in the conversion to the desired product (ESI S29†). This outcome provided additional evidence of the heterogeneity of Pd/SS-CNSs catalyst. The catalyst Pd/SS-CNSs in heterogeneous catalysis has the unique property that it is biowaste-derived and thus renewable. The catalytic system produced good results across a variety of substrates with low loadings of expensive Pd, and it exhibits promising potential with further research with respect to enhanced stabilization of Pd nanoparticles to further increase the recyclability.

The Table 3, which compares the Pd/SS-CNSs catalyst to several Pd-based recoverable catalysts for the Suzuki coupling of 4-bromophenol and phenylboronic acid, makes this comparison evident. The outcomes are shown in Table 3. According to the findings, the current catalyst looks to work better than certain other catalysts. Some catalyst systems that have been previously reported have longer durations, greater reaction temperatures, higher Pd loading or lower efficiencies. Also the detailed study of commerically Pd-supported on activated carbon (Pd/C) for the Suzuki–Miyaura coupling reactions have been investigated in other works.[48] It is noteworthy that elevated palladium concentrations, or the application of high temperature, microwave irradiation, longer duration and pressure, has conventionally been deemed essential for achieving effective reaction progress.[49] However, only a few studies have explored Suzuki–Miyaura coupling reactions without additives under milder conditions, catalyzed by Pd/C catalysts.[50,51] Consequently, the catalyst employed in the present study, Pd/SS-CNSs, synthesized using an activation-free technique, demonstrates
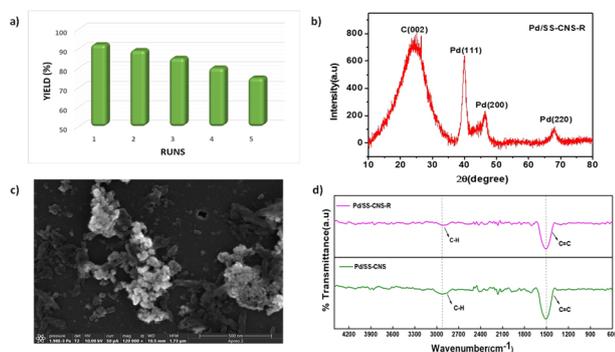

Fig. 7 Recyclability test of Pd/SS-CNSs (a), XRD pattern of (b), FESEM image (c) and FTIR spectra of the reused Pd/SS-CNSs (Pd/SS-CNS-R) (d).

Table 3 Comparison of the synthesized catalyst Pd/SS-CNSs with other reported heterogeneous catalysts containing palladium

| Entry	Catalyst	Palladium loading (mol%)	Experimental conditions	Yield (%)	Ref.
1	Pd/Fe@Fe$_x$O$_y$	5	K$_2$CO$_3$, EtOH/water 1 : 1, 70 °C, 4 h	60	40
2	Pd(0)·PzC	3	KOH, TBAB (tetrabutylammonium bromide), water, 90 °C, 2 h, under aerobic conditions	97	41
3	GO–Met–Pd	0.1	K$_2$CO$_3$, H$_2$O/EtOH, 60 °C, 5 h, under aerobic conditions	85	42
4	Pd/CNSs	10	Na$_2$CO$_3$, MeOH, 150 °C, 40 min, microwave assisted	99	29
5	Pd(II) salen@CPGO	0.7	K$_2$CO$_3$, DMF, 80 °C, 3 h	87	43
6	Fe$_3$O$_4$@MCM-41–CPS–TCH–Pd	0.186	K$_2$CO$_3$, EtOH : H$_2$O, 80 °C, 1 h	80	44
7	Pd@DTE	0.1	K$_2$CO$_3$, TBAB EtOH/water 1 : 1, 50 °C, 4 h, under aerobic conditions	98.4	45
8	Het–PG–NHC–Pd	1.6	K$_2$CO$_3$, DMF : H$_2$O (1 : 1), 80 °C, 3 h	87	46
9	BC–TPEA@Pd	1.0	(BERL : EtOH) (1 : 1), 70 °C 1 h	82	47
10	Pd/SS-CNSs	0.1	K$_2$CO$_3$, EtOH/water 2 : 1, 70 °C, 1 h, under aerobic conditions	96	This work
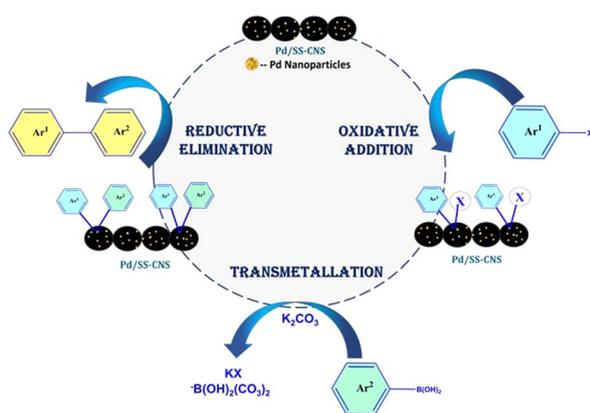
Fig. 8 Proposed mechanism for the Pd/SS-CNSs catalyst mediated Suzuki coupling reaction.

efficient catalysis under mild reaction conditions, with minimal use of precious palladium metal (0.1 mol%), making it a cost-effective option.

Catalytic mechanism

The carbon nanospheres like a majority of carbons exhibit high electron conductivity, promoting rapid electron transfer within their structure. This efficient electron conduction leads to better charge balance throughout the support as compared to other materials, resulting in stronger dipole–dipole interactions in the vicinity of a Pd-NPs. Additionally, the presence of pores and defects in the carbon structure may contribute to the electrostatic stabilization of Pd-NPs. Furthermore, the mesoporous carbon framework allows for effective steric confinement of the nanoparticles.[52,53] Following a comprehensive characterization of Pd/SS-CNSs, along with investigations into its stability, recyclability, and heterogeneity as a catalyst in Suzuki coupling, a plausible reaction mechanism is proposed and depicted in Fig. 8. In this proposed mechanism, aryl halides first undergo oxidative addition on the Pd nanoparticles immobilized on the surface of carbon nanospheres. Subsequently, they react with boronic acid

or its derivatives in the presence of a base, which activates the boronic acid and facilitates the transmetallation step. This leads to the formation of an intermediate (Ar^1–Pd–Ar^2). Finally, the formed intermediate (Ar^1–Pd–Ar^2) undergoes reductive elimination, resulting in the formation of a biaryl system (Ar^1–Ar^2).

Conclusions

The Pd/SS-CNSs catalyst was synthesized through a straightforward pyrolysis process utilizing biowaste, and the incorporation of Pd nanoparticles was achieved through an *in situ* reduction technique. The SS-CNSs exhibited substantial porosity and effectively incorporated approximately 3% of Pd. This innovative Pd/SS-CNSs catalyst demonstrated remarkable efficiency as a heterogeneous catalyst for Suzuki–Miyaura coupling reactions. The approach offers multiple advantages, including effective catalysis under mild reaction conditions, minimal utilization of precious palladium metal (0.1 mol%), reduced reaction times, and facile catalyst separation and cost effectiveness. These attributes stand in contrast to conventional homogeneous methods, reflecting the commitment to an environmentally conscious approach.

Moreover, the ligand-free nature of the catalyst prevents product contamination with residues of the ligands. The synthesized catalyst Pd/SS-CNSs therefore holds significant promise as an economically viable heterogeneous catalyst for Suzuki–Miyaura cross-coupling reactions, with potential applications extending to other Pd-catalyzed organic reactions. The current work also introduces a straightforward method for creating porous carbons from *Samanea saman* pods, which serve as supports for metal nanoparticles. The future objectives involve in enhancing the recyclability of the catalyst by stabilizing nanoparticles on porous carbons. Ongoing investigations are focused on expanding Pd-catalysis to other processes and exploring the immobilization of additional types of metal nanoparticles.

Author contributions

Apoorva Shetty: conceptualization, methodology, data curation, investigation, validation, writing – original draft, writing-review

& editing. Dhanya Sunil: data curation, resources. Thitima Rujiralai: validation, resources. Sanjeev Maradur: data curation, resources. Abdullah Alodhayb: validation, resources. Gurumurthy Hegde: conceptualization, methodology, supervision, validation, funding acquisition, writing-review & editing.

Conflicts of interest

There are no conflicts to declare.

Acknowledgements

Notes and references

1 C. P. Delaney, V. M. Kassel and S. E. Denmark, *ACS Catal.*, 2020, **10**, 73–80.

2 A.-M. Caminade and R. Laurent, *Coord. Chem. Rev.*, 2019, **389**, 59–72.

3 H. Veisi, M. Abrifam, S. A. Kamangar, M. Pirhayati, S. G. Saremi, M. Noroozi, T. Tamoradi and B. Karmakar, *Sci. Rep.*, 2021, **11**, 21883.

4 T. Baran and M. Nasrollahzadeh, *J. Phys. Chem. Solids*, 2020, **146**, 109566.

5 H. Jin, C. Zhang, P. Liu, X. Ge and S. Zhou, *Appl. Organomet. Chem.*, 2022, **36**(5), e6642.

6 P. Verma, Y. Kuwahara, K. Mori, R. Raja and H. Yamashita, *Nanoscale*, 2020, **12**, 11333–11363.

7 F. Habeche, M. Hachemaoui, A. Mokhtar, K. Chikh, F. Benali, A. Mekki, F. Zaoui, Z. Cherifi and B. Boukoussa, *J. Inorg. Organomet. Polym. Mater.*, 2020, **30**, 4245–4268.

8 F. Ghobakhloo, M. Mohammadi, M. Ghaemi and D. Azarifar, *ACS Appl. Nano Mater.*, 2024, **7**, 1265–1277.

9 M. Mohammadi, M. Khodamorady, B. Tahmasbi, K. Bahrami and A. Ghorbani-Choghamarani, *J. Ind. Eng. Chem.*, 2021, **97**, 1–78.

10 J. J. Torrez-Herrera, S. A. Korili and A. Gil, *Catal. Rev.*, 2022, **64**, 592–630.

11 V. I. Parvulescu and H. García, *Catal. Sci. Technol.*, 2018, **8**, 4834–4857.

12 E. Pérez-Mayoral, V. Calvino-Casilda and E. Soriano, *Catal. Sci. Technol.*, 2016, **6**, 1265–1291.

13 E. Lam and J. H. T. Luong, *ACS Catal.*, 2014, **4**, 3393–3410.

14 M. Mooste, E. Kibena-Põldsepp, V. Vassiljeva, M. Merisalu, M. Kook, A. Treshchalov, V. Kisand, M. Uibu, A. Krumme, V. Sammelselg and K. Tammeveski, *J. Mater. Sci.*, 2019, **54**, 11618–11634.

15 L. Nan, C. Yalan, L. Jixiang, O. Dujuan, D. Wenhui, J. Rouhi and M. Mustapha, *RSC Adv.*, 2020, **10**, 27923–27931.

16 H. Veisi, B. Karmakar, P. Mohammadi, T. Tamoradi, S. Hemmati and Z. Joshani, *Inorg. Chem. Commun.*, 2023, **156**, 110979.

17 S. U. Rather, *Int. J. Hydrogen Energy*, 2020, **45**, 4653–4672.

18 A. Mirabedini, Z. Lu, S. Mostafavian and J. Foroughi, *Nanomaterials*, 2020, **11**(1), 3.

19 A. Nieto-Márquez, R. Romero, A. Romero and J. L. Valverde, *J. Mater. Chem.*, 2011, **21**, 1664–1672.

20 Z. C. Kang and Z. L. Wang, *J. Phys. Chem.*, 1996, **100**, 5163–5165.

21 A. A. Deshmukh, S. D. Mhlanga and N. J. Coville, *Mater. Sci. Eng., R*, 2010, **70**, 1–28.

22 A. Nieto-Márquez, J. L. Valverde and M. A. Keane, *Appl. Catal., A*, 2009, **352**, 159–170.

23 A. N. Mohan and B. Manoj, *Int. J. Electrochem. Sci.*, 2012, **7**, 9537–9549.

24 N. Li, Y. Tong, H. Li, L. Wang, F. Hou, S. X. Dou and J. Liang, *Carbon*, 2021, **182**, 233–241.

25 P. Zhang, Z.-A. Qiao and S. Dai, *Chem. Commun.*, 2015, **51**, 9246–9256.

26 J. Tao, J. Zhou, Z. Yao, Z. Jiao, B. Wei, R. Tan and Z. Li, *Carbon*, 2021, **172**, 542–555.

27 L.-L. Pang, J.-Q. Bi, Y.-J. Bai, H.-L. Zhu, Y.-X. Qi, C.-G. Wang, F.-D. Han and S.-J. Li, *J. Phys. Chem. C*, 2008, **112**, 12134–12137.

28 X. Pei, Y. Li, L. Lu, H. Jiao, W. Gong and L. Zhang, *ACS Appl. Mater. Interfaces*, 2021, **13**, 44418–44426.

29 S. Supriya, G. S. Ananthnag, V. S. Shetti, B. M. Nagaraja and G. Hegde, *Appl. Organomet. Chem.*, 2020, **34**(3), e5384.

30 K. K. Raja, K. D. Srinivas and R. E. Raghava, *Int. J. Sci. Environ. Technol.*, 2017, 201599707.

31 O. J. Babayemi, O. J. Ifut, U. A. Inyang and L. J. Isaac, *Agric. J.*, 2010, **5**, 225–228.

32 D. C. Delgado, R. Hera, J. Cairo and Y. Orta, *Cuban J. Agric. Sci.*, 2014, **48**(3), 573.

33 M. Turáková, M. Králik, P. Lehocký, Ľ. Pikna, M. Smrčová, D. Remeteiová and A. Hudák, *Appl. Catal., A*, 2014, **476**, 103–112.

34 S. Yallappa, S. A. A. Manaf, M. J. A. Shiddiky, J. H. Kim, M. S. A. Hossain, V. Malgras, Y. Yamauchi and G. Hegde, *J. Nanosci. Nanotechnol.*, 2017, **17**, 2837–2842.

35 S. Supriya, G. S. Ananthnag, T. Maiyalagan and G. Hegde, *J. Cluster Sci.*, 2023, **34**, 243–254.

36 S. A. A. Manaf, P. Roy, K. V. Sharma, Z. Ngaini, V. Malgras, A. Aldalbahi, S. M. Alshehri, Y. Yamauchi and G. Hegde, *RSC Adv.*, 2015, **5**, 24528–24533.

37 S. Yallappa, D. R. Deepthi, S. Yashaswini, R. Hamsanandini, M. Chandraprasad, S. A. Kumar and G. Hegde, *Nano-Struct. Nano-Objects*, 2017, **12**, 84–90.

38 H.-J. Peng, G.-X. Hao, Z.-H. Chu, Y.-W. Lin, X.-M. Lin and Y.-P. Cai, *RSC Adv.*, 2017, **7**, 34104–34109.

39 P. Jerome, S. G. Babu and R. Karvembu, *Catal. Lett.*, 2021, **151**, 1633–1645.

40 A. Villacampa, L. Duque, O. Juanes, F. J. Palomares, P. Herrasti and N. Menéndez, *J. Mater. Sci.*, 2022, **57**, 241–253.

41 A. Verma, K. Tomar and P. K. Bharadwaj, *Inorg. Chem.*, 2019, **58**, 1003–1006.

42 S. Hemmati, L. Mehrazin, M. Pirhayati and H. Veisi, *Polyhedron*, 2019, **158**, 414–422.

43 M. Ghabdian, M. A. Nasseri, A. Allahresani and A. Motavallizadehkakhky, *Res. Chem. Intermed.*, 2021, **47**, 1713–1728.

44 A. Ahmadi, T. Sedaghat and R. Azadi, *J. Inorg. Organomet. Polym. Mater.*, 2021, **31**, 4126–4140.

45 Y. Qian, S. Y. Jeong, S.-H. Baeck, M.-J. Jin and S. E. Shim, *RSC Adv.*, 2019, **9**, 33563–33571.

46 J. K. Anjali and K. Sreekumar, *Catal. Lett.*, 2019, **149**, 1952–1964.

47 M. Kempasiddaiah, K. A. S. Raj, V. Kandathil, R. B. Dateer, B. S. Sasidhar, C. V. Yelamaggad, C. S. Rout and S. A. Patil, *Appl. Surf. Sci.*, 2021, **570**, 151156.

48 T. Maegawa, Y. Kitamura, S. Sako, T. Udzu, A. Sakurai, A. Tanaka, Y. Kobayashi, K. Endo, U. Bora, T. Kurita, A. Kozaki, Y. Monguchi and H. Sajiki, *Chemistry*, 2007, **13**, 5937–5943.

49 Z. Mao, H. Gu and X. Lin, *Catalysts*, 2021, **11**, 1078.

50 S.-Y. Liu, H.-Y. Li, M.-M. Shi, H. Jiang, X.-L. Hu, W.-Q. Li, L. Fu and H.-Z. Chen, *Macromolecules*, 2012, **45**, 9004–9009.

51 C. R. LeBlond, A. T. Andrews, Y. Sun and J. R. Sowa, *Org. Lett.*, 2001, **3**, 1555–1557.

52 B. V. Vaerenbergh, J. Lauwaert, P. Vermeir, J. De Clercq and J. W. Thybaut, in *Advances in Catalysis*, ed. C. Song, Academic Press, 2019, vol. 65, pp. 1–120.

53 A. Cao, R. Lu and G. Veser, *Phys. Chem. Chem. Phys.*, 2010, **12**, 13499–13510.